[C−H···O] Interactions as a Control Element in Supramolecular Complexes: Experimental and Theoretical Evaluation of Receptor Affinities for the Binding of Bipyridinium-Based Guests by Catenated Hosts[1]

K. N. Houk,*,† Stephan Menzer,‡ Simon P. Newton,§ Françisco M. Raymo,†,§ J. Fraser Stoddart,*,†,§ and David J. Williams*,‡

Contribution from the Department of Chemistry and Biochemistry, University of California, 405 Hilgard Avenue, Los Angeles, California 90095-1569, School of Chemistry, University of Birmingham, Edgbaston, Birmingham B15 2TT, U.K., and Department of Chemistry, Imperial College, South Kensington, London SW7 2AY, U.K.

Received August 3, 1998

Abstract: Macrocyclic receptors incorporating two facing π-electron-rich aromatic surfaces, held at a distance of approximately 7 Å by polyether spacers, bind bipyridinium-based guests. This recognition motif, which is dictated by $\pi-\pi$ stacking and [C−H···O] hydrogen-bonding interactions, has led to the development of efficient template-directed syntheses of mechanically interlocked molecules, such as catenanes and rotaxanes. By employing a supramolecularly assisted synthetic methodology based on these interactions, we have self-assembled two novel [3]catenanes, each incorporating two 1,5-dioxynaphtho-38-crown-10 components and one bipyridinium-based tetracationic cyclophane component. Single-crystal X-ray analyses of these [3]catenanes revealed that they possess internal cavities bounded on two opposite sites by π-electron-rich 1,5-dioxynaphthalene units separated by a distance of approximately 7−8 Å. Despite the presence of apparently ideal "binding pockets", these mechanically interlocked compounds steadfastly refuse to bind bipyridinium-based guests in solution, as demonstrated by both ^{1}H NMR and UV−vis spectroscopy. AMBER* and HF/3-21G calculations on appropriate models show that the absence of [C−H···O] hydrogen-bonding interactions is responsible for the instability of these geometrically ideal complexes. The [C−H···O] bond appears to be quantitatively much more important than $\pi-\pi$ stacking interactions in these particular systems.

Introduction

The efficient template-directed syntheses[2] of [2]- and [3]catenanes, incorporating π-electron-rich and π-electron-deficient aromatic residues, rely principally upon the stabilizing and cooperative effects of $\pi-\pi$ stacking,[3] [C−H···O] hydrogen-bonding,[4] and [C−H···π] interactions.[5] The bipyridinium-based tetracationic cyclophanes cyclobis(paraquat-*p*-phenylene)[6] and cyclobis(paraquat-4,4′-biphenylene)[7] self-assemble[8] around one and two π-electron-rich dioxyarene rings, affording [2]- and [3]catenanes, respectively, when the π-electron-rich recognition sites are incorporated within macrocyclic polyethers. From the inspection of CPK space-filling molecular models, the obvious progression to [4]catenanes (Figure 1) incorporating two macrocyclic polyethers and two tetracationic cyclophane components appears simply to require the insertion of a third *p*-phenylene ring into each of the neutral spacers separating the

* Corresponding authors. Address correspondence to either K.N.H. or J.F.S. at the University of California.

† University of California.

‡ Imperial College.

§ University of Birmingham.

(1) Molecular Meccano. 47. For part 46, see: Ashton, P. R.; Ballardini, R.; Balzani, V.; Baxter, I.; Credi, A.; Fyfe, M. C. T.; Gandolfi, M. T.; Gómez-López, M.; Martinez-Diaz, M.-V.; Piersanti, A.; Spencer, N.; Stoddart, J. F.; Venturi, V.; White, A. J. P.; Williams, D. J. *J. Am. Chem. Soc.* **1998**, *120*, 11932−11942.

(2) For accounts and reviews on the template-directed syntheses of catenanes incorporating complementary π-electron-rich and π-electron-deficient components, see: (a) Gillard, R. E.; Raymo, F. M.; Stoddart, J. F. *Chem.—Eur. J.* **1997**, *3*, 1933−1940. (b) Fyfe, M. C. T.; Stoddart, J. F. *Acc. Chem. Res.* **1997**, *30*, 393−401. (c) Raymo, F. M.; Stoddart, J. F. *Chemtracts* **1998**, *11*, 491−511. (d) Hamilton, D. G.; Davies, J. E.; Prodi, L.; Sanders, J. K. M. *Chem.—Eur. J.* **1998**, *4*, 608−620.

(3) For accounts and reviews on $\pi-\pi$ stacking interactions, see: (a) Hunter, C. A.; Sanders, J. K. M. *J. Am. Chem. Soc.* **1990**, *112*, 5525−5534. (b) Hunter, C. A. *Angew. Chem., Int. Ed. Engl.* **1993**, *32*, 1584−1586. (c) Cozzi, F.; Siegel, J. S. *Pure Appl. Chem.* **1995**, *67*, 683−689. (d) Shetty, A. S.; Zhang, J.; Moore, J. S. *J. Am. Chem. Soc.* **1996**, *118*, 1019−1027.

(4) For accounts and reviews on [C−H···O] hydrogen-bonding interactions, see: (a) Desiraju, G. R. *Acc. Chem. Res.* **1991**, *24*, 290−296. (b) Desiraju, G. R. *Acc. Chem. Res.* **1996**, *29*, 441−449. (c) Krishnamohan Sharma, C. V.; Zaworotko, M. J. *Chem. Commun.* **1996**, 2655−2656. (d) Steiner, T. *Chem. Commun.* **1997**, 727−734. (e) Berger, I.; Egli, M. *Chem.—Eur. J.* **1997**, *3*, 1400−1404. (f) Bodige, S. G.; Rogers, R. D.; Blackstock, S. C. *Chem. Commun.* **1997**, 1669−1670.

(5) For accounts and reviews on [C−H···π] interactions, see: (a) Nishio, M.; Umezawa, Y.; Hirota, M.; Takeuchi, Y. *Tetrahedron* **1995**, *51*, 8665−8701. (b) Umezawa, Y.; Tsuboyama, S.; Honda, K.; Uzawa, J.; Nishio, M. *Bull. Chem. Soc. Jpn.* **1998**, *71*, 1207−1213. (c) Nishio, M.; Hirota, M.; Umezawa, Y. *The [C−H···π] Interaction. Evidence, Nature, and Consequences*; Wiley: New York, 1998.

(6) (a) Anelli, P. L.; Ashton, P. R.; Ballardini, R.; Balzani, V.; Delgado, M.; Gandolfi, M. T.; Goodnow, T. T.; Kaifer, A. E.; Philp, D.; Pietraszkiewicz, M.; Prodi, L.; Reddington, M. V.; Slawin, A. M. Z.; Spencer, N.; Stoddart, J. F.; Vicent, C.; Williams, D. J. *J. Am. Chem. Soc.* **1992**, *114*, 193−218. (b) Asakawa, M.; Dehaen, W.; L'abbé, G.; Menzer, S.; Nouwen, J.; Raymo, F. M.; Stoddart, J. F.; Williams, D. J. *J. Org. Chem.* **1996**, *61*, 9591−9595.

(7) (a) Asakawa, M.; Ashton, P. R.; Menzer, S.; Raymo, F. M.; Stoddart, J. F.; White, A. J. P.; Williams, D. J. *Chem.—Eur. J.* **1996**, *2*, 877−893. (b) Ashton, P. R.; Menzer, S.; Raymo, F. M.; Shimizu, G. K. H.; Stoddart, J. F.; Williams, D. J. *Chem. Commun.* **1996**, 487−490.

10.1021/ja982748b CCC: $18.00
Published on Web 02/09/1999

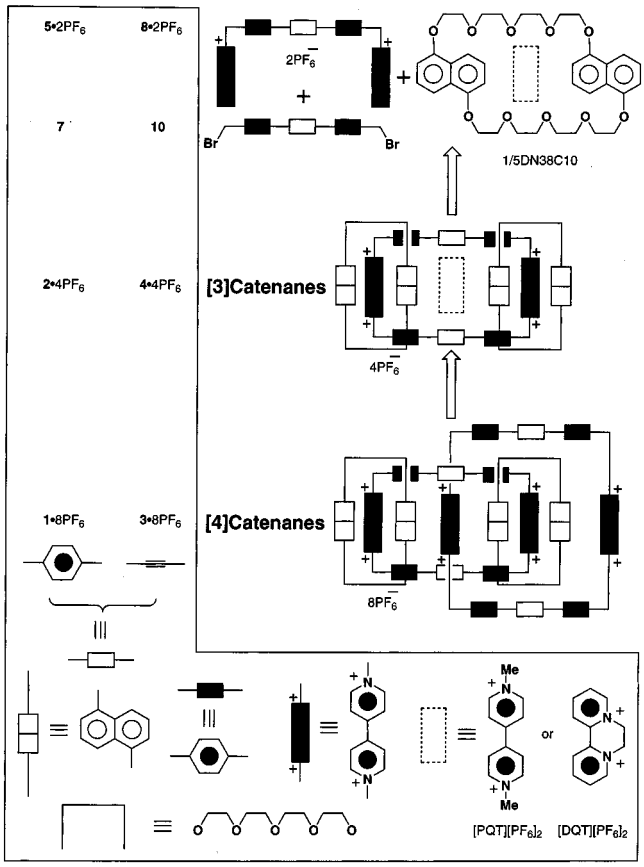

Figure 1. Retrosynthetic analysis of [4]catenanes each incorporating two macrocyclic polyethers and two tetracationic cyclophanes. Note the similarities between the cavities of the macrocyclic polyether 1/5DN38C10 and the [3]catenanes **2**·4PF$_6$ and **4**·4PF$_6$.

two bipyridinium units to give cyclobis(paraquat-4,4′-terphenylene). Thus, the self-assembly of the [4]catenane **1**·8PF$_6$ should occur after the formation of the [3]catenane intermediate **2**·4PF$_6$ which possesses a cavity large enough to permit the catenation of a fourth ring. However, all our numerous attempts to self-assemble the [4]catenane **1**·8PF$_6$ by conventional template-directed approaches have so far failed. The compound that did result from the attempted template-directed synthesis was the [3]catenane **2**·4PF$_6$. Similarly, when the central phenylene ring of the terphenylene units present in the reactants and products is replaced by an acetylenic linkage, the outcome is exactly the same—namely, the [4]catenane **3**·8PF$_6$ is not formed and it is the [3]catenane **4**·4PF$_6$ which is isolated. Furthermore, the [3]catenanes **2**·4PF$_6$ and **4**·4PF$_6$ do not bind the π-electron-deficient bipyridinium-based substrates paraquat bis(hexafluorophosphate), [PQT][PF$_6$]$_2$, and diquat bis(hexafluorophosphate), [DQT][PF$_6$]$_2$ (Figure 1), in solution. By contrast, the macrocyclic polyether 1/5DN38C10, which possesses a sterically accessible π-electron-rich cavity remarkably similar to those of the [3]catenanes, strongly binds [PQT][PF$_6$]$_2$ and [DQT][PF$_6$]$_2$. In this paper, we report the experimental details for the formation of the [3]catenanes **2**·4PF$_6$ and **4**·4PF$_6$ and attempt to explain the failure to obtain the [4]catenanes **1**·8PF$_6$ and **3**·8PF$_6$. The analyses of the crystal structures, combined with conformational analyses using force field and ab initio quantum mechanical calculations, have shown that the combined strength of numerous [C−H···O] hydrogen bonds can be remarkably large and indeed much greater than π···π stacking effects. Previous suggestions[6,9] of the importance of [C−H···O] hydrogen bonding in related systems have not provided quantitative measures of the magnitude of these interations. Here, we report an example where complex formation cannot occur in the absence of [C−H···O] hydrogen bonding. The role of [C−H···O] hydrogen bonding in biological systems and self-assembly continues to receive increasing recognition and acceptance.[4]

Scheme 1

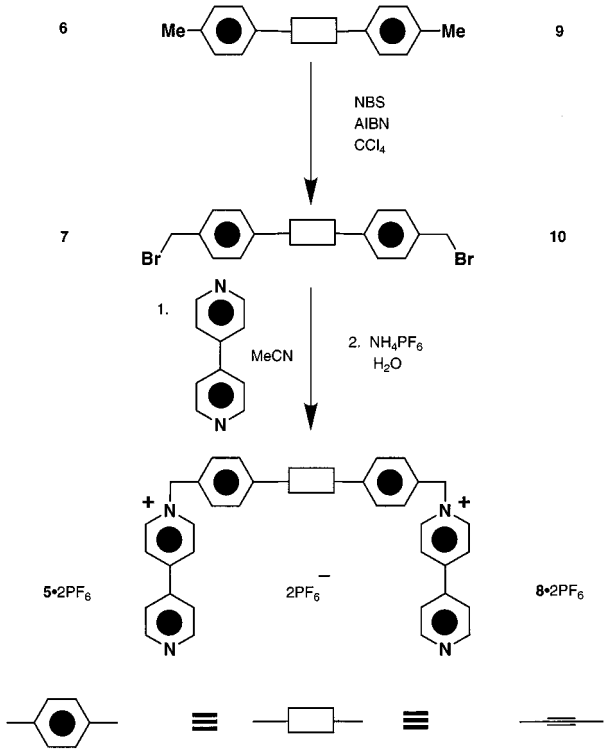

Results and Discussion

[3]Catenane 2·4PF$_6$ Incorporating Cyclobis(paraquat-4,4′-terphenylene). The salt **5**·2PF$_6$ was synthesized (Scheme 1) in two steps. Bromination of 4,4′-dimethyl-1,4-terphenyl, **6**, afforded the dibromide **7**, which was reacted subsequently with 4,4′-bipyridine to give **5**·2PF$_6$ in a yield of 75%, after counterion exchange. Reaction (Scheme 2) of **5**·2PF$_6$ with **7** in the presence of the macrocyclic polyether 1,5-dinaphtho-38-crown-10 (1/5DN38C10) gave the [3]catenane **2**·4PF$_6$—incorporating *two* macrocyclic polyethers and *one* tetracationic cyclophane component—in a yield of 5% after counterion exchange. Surprisingly, the expected [4]catenane **1**·8PF$_6$—incorporating *two* macrocyclic polyethers and *two* tetracationic cyclophane components—was not formed. Even when the reaction was repeated using ultrahigh-pressure conditions (12 kbar), only the [3]catenane **2**·4PF$_6$ was isolated, this time in the slightly better yield of 10%.

(8) For accounts and reviews on self-assembly processes, see: (a) Stoddart, J. F. in *Chirality in Drug Design and Synthesis*; Brown, C., Ed.; Academic Press: London, 1990; pp 53−81. (b) Mallouk, T. E.; Lee, H. *J. Chem. Educ.* **1990**, *67*, 829−834. (c) Constable, E. C. *Angew. Chem., Int. Ed. Engl.* **1991**, *30*, 1450−1451. (d) Lindsey, J. S. *New J. Chem.* **1991**, *15*, 153−180. (e) Menger, F. M.; Lee, S. S.; Tao, X. *Adv. Mater.* **1995**, *7*, 669−671. (f) Ghadiri, M. R. *Adv. Mater.* **1995**, *7*, 675−677. (g) Hunter, C. A. *Angew. Chem., Int. Ed. Engl.* **1995**, *34*, 1079−1081. (h) Lawrence, D. S.; Jiang, T.; Levett, M. *Chem. Rev.* **1995**, *95*, 2229−2260. (i) Raymo, F. M.; Stoddart, J. F. *Curr. Opin. Colloid Interface Sci.* **1996**, *1*, 116−126. (j) Philp, D.; Stoddart, J. F. *Angew. Chem., Int. Ed. Engl.* **1996**, *35*, 1154−1196.

(9) (a) Castro, R.; Nixon, K. R.; Evanseck, J. D.; Kaifer, A. E. *J. Org. Chem.* **1996**, *61*, 7298−7303. (b) Asakawa, M.; Brown, C. L.; Menzer, S.; Raymo, F. M.; Stoddart, J. F.; Williams D. J. *J. Am. Chem. Soc.* **1997**, *119*, 2614−2627.

Scheme 2

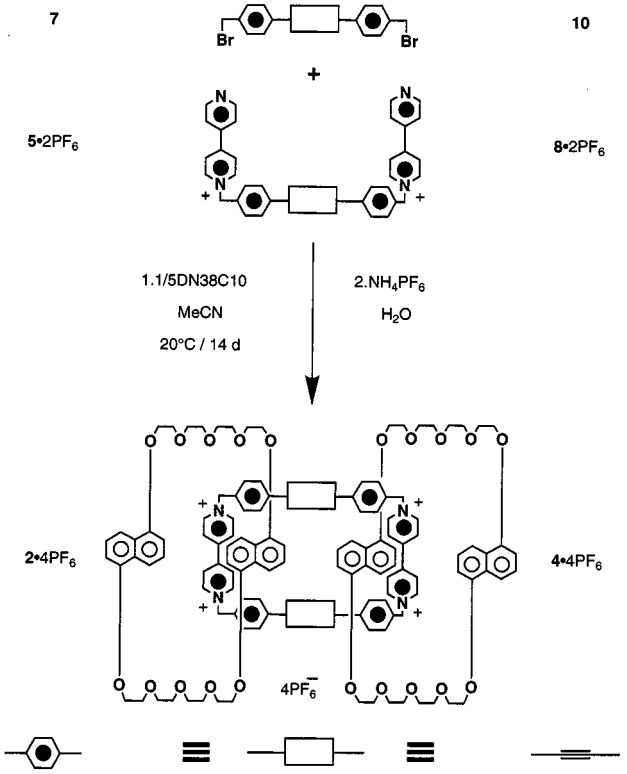

The [3]catenane **2**·4PF_6 was characterized unequivocally by low- and high-resolution liquid secondary ion mass spectrometry (LSIMS), ^{1}H NMR spectroscopy, and X-ray crystallographic analysis. The LSIMS spectrum revealed three peaks centered on *m*/*z* 2534, 2389, and 2244 for $[M - PF_6]^+$, $[M - 2PF_6]^+$, and $[M - 3PF_6]^+$, respectively, corresponding to the losses of one, two, and three PF_6^- counterions, respectively. The ^{1}H NMR spectrum recorded in CD_3CN at 350 K shows sharp and well-resolved signals for the π-electron-rich and the π-electron-deficient macrocyclic components. In particular, only one set of signals is observed for each pair of naphthalene protons, indicating that the circumrotation of the macrocyclic polyethers through the cavity of the tetracationic cyclophane is fast on the ^{1}H NMR time scale at 350 K. Similarly, the protons located in the α- and β-positions, with respect to the nitrogen atoms, on the bipyridinium units resonate as two doublets only—i.e., the local C_{2h} symmetry which could be imposed by the 1,5-dioxynaphthalene units is "lost" at this temperature as a result of the fast dynamic processes on the ^{1}H NMR time scale involving their exchange or reorientation.[10] On cooling of the CD_3CN solution of the [3]catenane down to 290 and then to 253 K, the circumrotation of the π-electron-rich through the π-electron-deficient macrocyclic components becomes slow and significant broadening of the resonances associated with the naphthalene and bipyridinium protons is observed. Unfortunately, as a result of the very low solubility of the [3]catenane in solvents having freezing points lower than that of CD_3CN, ^{1}H NMR spectra of **2**·4PF_6 at temperatures lower than 253 K could not be recorded, thus preventing the determination of the energy barrier associated with this circumrotation process.

The single-crystal X-ray analysis of the [3]catenane **2**·4PF_6 shows (Figure 2) that the molecule has crystallographic C_i symmetry, with the two 1,5-dinaphtho-38-crown-10 rings—each of which have local D_2 symmetry—encircling the bipyridinium units of the extended tetracationic cyclophane. This molecular geometry is stabilized by a combination[11] of $\pi-\pi$ stacking, [C−H···O] hydrogen-bonding, and [C−H···π] interactions, similar to those observed[2] in analogous [2]- and [3]catenanes. A consequence of the local D_2 symmetry of each macrocyclic polyether component is a marked difference in the inclination of the O···O vectors of the 1,5-dioxynaphthalene rings with respect to the N···N axes of the encircled bipyridinium units. The "inside" O···O vector is inclined by 124°, while the "alongside" O···O vector is inclined by only 10° to the N···N axes. The tetracationic cyclophane displays a rigid open geometry with a length (between the bipyridinium units) of ca. 15.10 Å and a breadth (between the centroids of the middle phenylene rings of the terphenyl linkages) of 11.20 Å. A key parameter of this molecular structure is the size of the void formed between the two inside 1,5-dioxynaphthalene residues: the mean interplanar separation is 7.93 Å, a distance that is ca. 0.9 Å greater than the separation observed between the 1,5-dioxynaphthalene residues within each 1/5DN38C10 macrocycle.

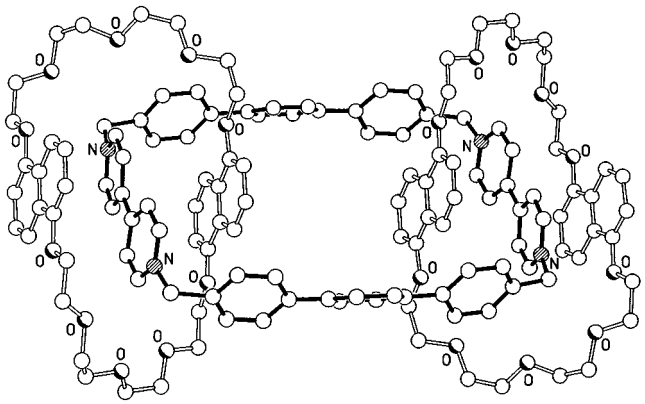

Figure 2. X-ray crystal structure of the [3]catenane **2**·4PF_6.

Inspection of the packing of the [3]catenane molecules revealed an absence of any intercatenane $\pi-\pi$ stacking interactions involving the bipyridinium units. However, symmetry-related tetracationic cyclophanes in the crystallographic *c* direction have their mean planes inclined by ca. 76° and are arranged such that the end phenyl rings of each terphenylene spacer are $\pi-\pi$ stacked with their symmetry-related counterparts to create (Figure 3) a folded mosaic-like array. The associated interplanar separations and centroid−centroid distances are 3.50 and 3.80 Å, respectively.

The cavity within the [3]catenane **2**·4PF_6 is lined by the π-electron-rich 1,5-dioxynaphthalene units and is large enough, at least in principle, to accommodate π-electron-deficient guests such as $[PQT][PF_6]_2$ and $[DQT][PF_6]_2$. However, the ^{1}H NMR spectra of equimolar CD_3CN solutions of the [3]catenane with either $[PQT][PF_6]_2$ or $[DQT][PF_6]_2$ did not show any significant

(10) (a) Asakawa, M.; Ashton, P. R.; Boyd, S. E.; Brown, C. L.; Gillard, R. E.; Kocian, O.; Raymo, F. M.; Stoddart, J. F.; Tolley, M. S.; White, A. J. P.; Williams, D. J. *J. Org. Chem.* **1997**, *62*, 26−37. (b) Bravo, J. A.; Raymo, F. M.; Stoddart, J. F.; White, A. J. P.; Williams, D. J. *Eur. J. Org. Chem.* **1998**, 2565−2571.

(11) The mean interplanar separations between both the "inside" and "alongside" 1,5-dioxynaphthalene residues and the bipyridinium unit are in each case 3.5 Å. There are [C−H···O] hydrogen bonds (i) between one of the hydrogen atoms in the α-positions with respect to the nitrogen atoms on the bipyridinium units and a central polyether oxygen atom ([C···O], 3.38 Å; [H···O], 2.46 Å; [C−H···O], 161°) and (ii) between one of the methylene groups of the tetracationic cyclophane and the adjacent oxygen atom of the same polyether linkage ([C···O], 3.30 Å: [H···O], 2.45 Å; [C−H···O], 148°). Additionally, there are edge-to-face [C−H···π] interactions involving the hydrogen atoms in the 4- and 8-positions of the "inside" 1,5-dioxynaphthalene residues and the proximal *p*-phenylene rings of the tetracationic cyclophane (respectively: [H···π], 2.73 and 2.82 Å; [C−H···π], 145 and 141°).

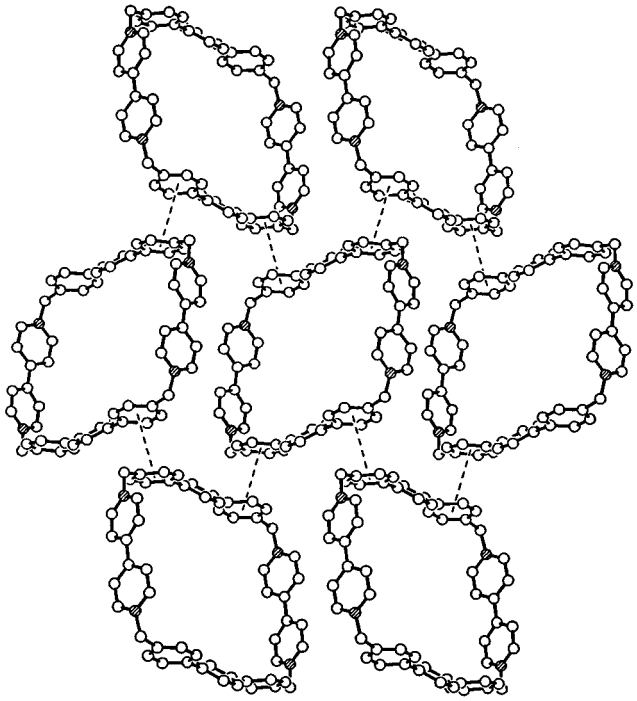

Figure 3. Packing diagram of the [3]catenane **2**·4PF_6. The macrocyclic polyether components have been omitted for clarity.

difference from the ^{1}H NMR spectra of the separate compounds, even at temperatures as low as 253 K—i.e., the lowest temperature at which an ^{1}H NMR spectrum of the [3]catenane **2**·4PF_6 can be recorded (vide supra). Similarly, even when a 5-fold excess of the "potential" guest was employed, no changes in the ^{1}H NMR spectra were detected. Consistently, the UV−vis spectra of the same solutions did not reveal any changes in the absorbance and/or wavelength of the charge-transfer band associated with the intracatenane donor−acceptor interactions. In addition, we attempted also to "catenate" the [3]catenane **2**·4PF_6 with a second cyclobis(paraquat-4,4′-terphenylene) tetracation by treating **2**·4PF_6 with an excess of **5**·2PF_6 and **7** in the hope of generating the [4]catenane **1**·8PF_6. However, only the original [3]catenane **2**·4PF_6 and some polymeric material resulting from the reaction of the **5**·2PF_6 with **7** were isolated from the reaction mixture. These results show that, contrary to reasonable expectations, the complexation of a π-electron-deficient guest "inside" the cavity of the [3]catenane **2**·4PF_6 does not occur. It was noted, however, that the separation between the "inside" 1,5-dioxynaphthalene units—i.e., the distance between the recognition sites lining the cavity of the potential receptor—might be too large, judging by the solid-state structure at least. It was, therefore, decided to try shortening the distance between the two bipyridinium units in the tetracationic cyclophane component by replacing the central phenylene ring in both terphenylene units by an acetylenic linkage in the hope of generating a [3]catenane possessing an internal cavity of a more appropriate size for the binding of π-electron-deficient guests.

The [3]Catenane 4·4PF_6 Incorporating Cyclobis(paraquat-4,4′-tolan). The salt **8**·2PF_6 incorporating a tolan spacer was prepared (Scheme 1) in two steps. The bromination of **9** was followed by the reaction of the resulting dibromide **10** with 4,4′-bipyridine, affording **8**·2PF_6 in a yield of 50%, after counterion exchange. The reaction (Scheme 2) of **8**·2PF_6 with **10** in the presence of the macrocyclic polyether 1/5DN38C10 afforded a [2]catenane—incorporating *one* macrocyclic polyether and *one* tetracationic cyclophane component—in addition to the [3]catenane **4**·4PF_6 in yields of 10 and 35%, respectively, after counterion exchange. Again, the desired [4]catenane **3**·8PF_6 was not formed. Similarly, when the reaction was performed under ultrahigh-pressure conditions (12 kbar), the [3]catenane **4**·4PF_6 was isolated in a yield of 42%, together with trace amounts of the [2]catenane. Again no [4]catenane was detected.

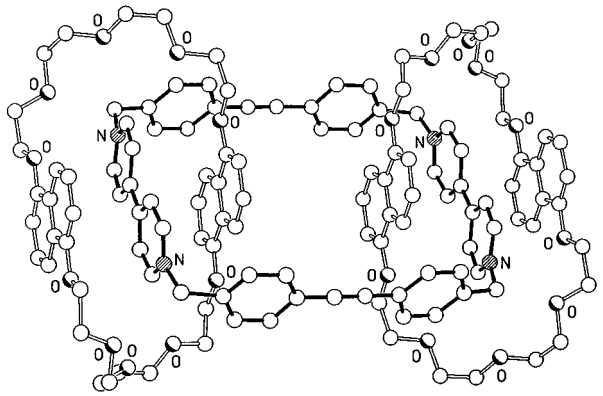

Figure 4. X-ray crystal structure of the [3]catenane **4**·4PF_6.

The [3]catenane **4**·4PF_6 was characterized by LSIMS, ^{1}H NMR spectroscopy, and X-ray crystallography. In addition to the molecular ion peak at *m*/*z* 2574 for $[M]^+$, the LSIMS spectrum of **4**·4PF_6 showed three peaks centered on *m*/*z* 2429, 2284, and 2139 for $[M - PF_6]^+$, $[M - 2PF_6]^+$, and $[M - 3PF_6]^+$, respectively, corresponding to the losses of one, two, and three PF_6^- counterions, respectively. The ^{1}H NMR spectrum of the [3]catenane **4**·4PF_6, recorded in $(CD_3)_2CO/CD_3NO_2$ (9:1, v/v) at 300 K, revealed only one set of signals for the three pairs of naphthalene protons. In addition, the protons in the α- and β-positions with respect to the nitrogen atoms on the bipyridinium units resonate as two doublets only. As before, the relative simplicity of this spectrum is a result of circumrotations of the macrocyclic polyethers through the cavity of the tetracationic cyclophane which are fast on the ^{1}H NMR time scale at room temperature. Thus, the "inside" and "alongside" 1,5-dioxynaphthalene units give rise to only one set of signals and cannot be distinguished. On cooling of the solution down to 280 K, the rate of the circumrotation process becomes slower and significant broadening of all signals is observed in the ^{1}H NMR spectrum. Further cooling to 210 K results in a more complex ^{1}H NMR spectrum which now shows two distinct sets of signals for the "inside" and "alongside" 1,5-dioxynaphthalene units. In particular, NOE experiments revealed that the protons $H_{4/8}$ of the "inside" 1,5-dioxynaphthalene units resonate at δ 4.15. In addition, the resonances associated with the protons in the α-positions with respect to the nitrogen atoms on the bipyridinium units separate into two sets of signals as a result of the local C_{2h} symmetry of the 1,5-dioxynaphthalene units. By employment of the approximate coalescence treatment,[12] a free energy barrier of 12.5 kcal mol^{-1} was determined for the circumrotation process at the coalescence temperature (280 K) of the probe $H_{4/8}$ protons of the 1,5-dioxynaphthalene units.

The single-crystal X-ray analysis of the [3]catenane **4**·4PF_6 revealed (Figure 4) a C_i symmetric structure very similar to that observed for **2**·4PF_6, though with the desired shortening of the dimensions of the tetracationic cyclophane and hence of the separation of the "inside" 1,5-dioxynaphthalene units. The length of the cyclophane is reduced to 13.47 Å, whereas the breadth is unchanged at 11.15 Å. The accompanying interplanar

(12) (a) Sutherland, I. O. *Annu. Rep. NMR Spectrosc.* **1971**, *4*, 71−235. (b) Sandström, J. *Dynamic NMR Spectroscopy*; Academic Press: London, 1982.

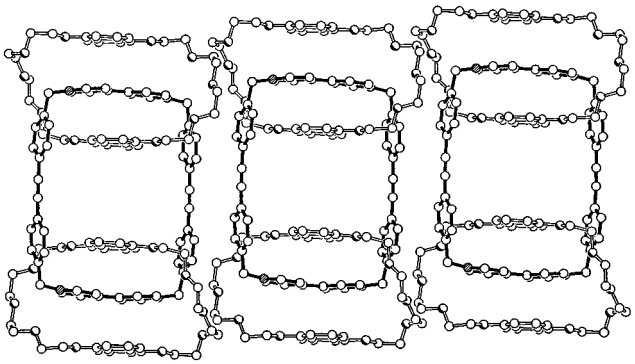

Figure 5. Packing diagram of the [3]catenane **2**·4PF_6.

separation between the "inside" dioxynaphthalene rings is reduced to 6.77 Å, a value which should be near optimal for the insertion of a π-electron-deficient guest. The replacement of the terphenylene by tolan units within the tetracationic cyclophane component is also accompanied by a marked change in the conformation of one of the polyether linkages which results in a minor alteration in the relative tilts of the O···O vectors of the "inside" and "alongside" 1,5-dioxynaphthalene residues with respect to the N···N axes of the encircled bipyridinium units: the "inside" O···O vector is inclined by 128° while the "alongside" O···O vector is inclined by only 5°; cf. 124 and 10°, respectively in **2**·4PF_6. Stabilization is again achieved via a combination of $\pi-\pi$, [C−H···O], and [C−H···π] interactions.[13] The [3]catenane molecules form extended stacks (Figure 5) with the planes of the acetylenic spacers of adjacent lattice-translated molecules being ca. 3.28 Å apart; the shortest intermolecular atom−atom contact is 3.43 Å between one of the acetylenic carbon atoms of one molecule and one of the quaternary aromatic carbon atoms in the diphenylacetylenic spacer of the next and vice versa.

Despite this "optimization" of the distance separating the π-electron-rich 1,5-dioxynaphthalene recognition sites lining the cavity of the [3]catenane, again, no complexation of either [PQT][PF_6]$_2$ or [DQT][PF_6]$_2$ was detected by ^{1}H NMR spectroscopy even at temperatures as low as 210 K. Binding experiments were also carried out with neutral π-electron-deficient guests, such as 1,4-benzoquinone and perfluorohydroquinone as alternatives to the positively charged [PQT][PF_6]$_2$ and [DQT][PF_6]$_2$ guests. However, no changes in the chemical shifts or in the absorbance and/or wavelength of the charge-transfer band associated with the [3]catenane were detected by ^{1}H NMR and UV−vis spectroscopies, respectively.

Computational Evaluation of Binding Interactions. The π-electron-rich macrocyclic polyether 1/5DN38C10 binds[10,14] the π-electron-deficient bipyridinium salt $[PQT]^{2+}$ in solution (K_a = 1190 M^{-1} in CD_3CN at 25 °C) and in the solid state.

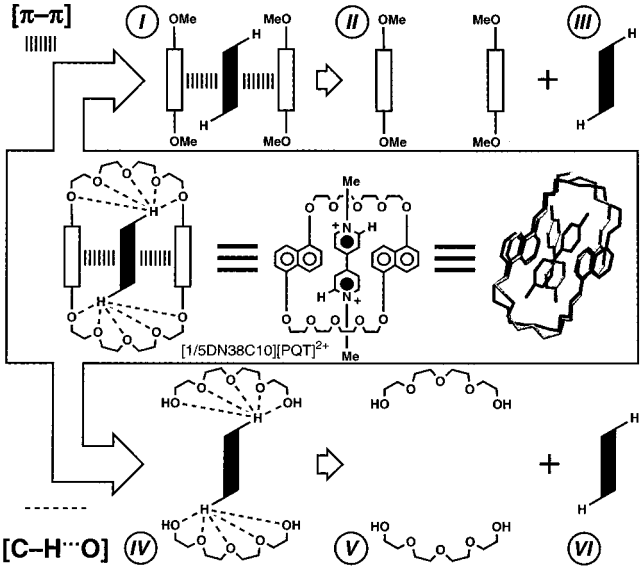

Figure 6. Fragmentation of the complex $[1/5DN38C10][PQT]^{2+}$ performed in order to "isolate" the [C−H···O] hydrogen bonds from the $\pi-\pi$ stacking interactions as well as the superimposed (black) solid-state and (gray) calculated (simulated annealing, AMBER* force field) geometries of the complex.

The single-crystal X-ray analysis of the corresponding complex revealed (Figure 6) a pseudorotaxane geometry with the bipyridinium unit of the guest sandwiched between the 1,5-dioxynaphthalene units of the host. In addition, short distances between the acidic hydrogen atoms in the α-positions with respect to the nitrogen atoms on the bipyridinium units and some of the polyether oxygen atoms were also noted. These observations suggested that the formation of this complex is a result of $\pi-\pi$ stacking interactions between the complementary aromatic units as well as of [C−H···O] hydrogen bonds. This solid-state geometry was used as the input structure for a simulated annealing molecular dynamics study using the AMBER* force field[15] in conjunction with the GB/SA solvation model[16] for H_2O, as implemented in Macromodel.[17] The calculated and solid-state geometries differ (Figure 6) significantly in the relative orientation of the aromatic units of host and guest. In the calculated structure, the angles between the N···N axis of the bipiridinium unit of the guest and the O···O axes of the 1,5-dioxynaphthalene units of the host are 126 and 138° whereas, in the centrosymmetric solid-state structure, the angle is 19°. To analyze the effect that the relative orientation of the complementary aromatic units has upon the binding energy, the model dimer complex shown in Figure 7a was employed. This complex was constructed with Spartan[18] by orienting the bipyridinium and 1,5-dioxynaphthalene units parallel to each other with a centroid−centroid separation[19] of 3.51 Å. The angle θ was varied from 0 to 180° in consecutive steps of 10° each,

(13) The mean interplanar separations between both the "inside" and "alongside" 1,5-dioxynaphthalene residues and the bipyridinium unit are 3.33 and 3.35 Å. There are [C−H···O] hydrogen bonds (i) between diametrically opposite pairs of hydrogen atoms located in the α-positions with respect to the nitrogen atoms on the bipyridinium units and the oxygen atoms in the proximal polyether linkages (respectivley: [C···O], 3.26, 3.30, and 3.23 Å; [H···O], 2.43, 2.44, and 2.45 Å; [C−H···O], 145, 148, and 138°) and (ii) between one of the methylene groups of the tetracationic cylophane and one of the oxygen atoms in one of the polyether linkages ([C···O], 3.12 Å; [H···O], 2.39 Å; [C−H···O], 133°). Additionally, there are two edge-to-face [C−H···π] interactions involving the "inside" 1,5-dioxynaphthalene residues and the proximal *p*-phenylene rings of the tetracationic cyclophane ([H···π], 2.72 and 2.76 Å; [C−H···π], 148 and 145°).

(14) Ashton, P. R.; Chrystal, E. J. T.; Mathias, J. P.; Parry, K. P.; Slawin, A. M. Z.; Spencer, N.; Stoddart, J. F.; Williams, D. J. *Tetrahedron Lett.* **1987**, *28*, 6367−6370.

(15) Weiner, S. J.; Kollman, P. A.; Case, D. A.; Singh, V. C.; Ghio, C.; Alagona, G.; Profeta, S., Jr.; Weiner, P. *J. Am. Chem. Soc.* **1984**, *106*, 765−784.

(16) Still, W. C.; Tempczyk, A.; Hawley, R. C.; Hendrickson, T. *J. Am. Chem. Soc*. **1990**, *112*, 6127−6129.

(17) Mohamadi, F.; Richards, N. G. J.; Guida, W. C.; Liskamp, R.; Lipton, M.; Caufield, C.; Chang, G.; Hendrickson, T.; Still, W. C. *J. Comput. Chem.* **1990**, *11*, 440−467.

(18) *Spartan 4.1*; Wavefunction Inc.: 18401 Von Karman Ave., 370 Irvine, CA 92715.

(19) A statistical survey of the Cambridge Crystallographic Database (Allen, F. H.; Davies, J. E.; Galloy, J. J.; Johnson, O.; Kennard, P.; Macrae, C. F.; Watson D. G. *J. Chem. Inf. Comput. Sci.* **1991**, *31*, 187−204) revealed that the average centroid−centroid separation between stacked 1,5-dioxynaphthalene and bipyridinium units is 3.51 Å.

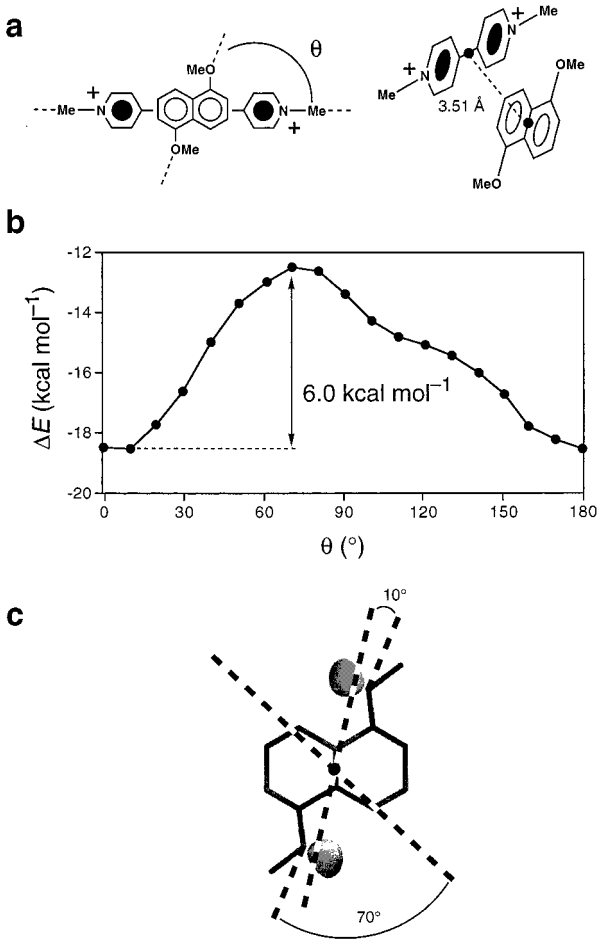

Figure 7. (a) The model dimer complex employed to evaluate the effect of the relative orientation of the aromatic units on the binding energy. (b) Plot of the calculated (HF/3-21G*) binding energies of the model dimer complex against the angle θ. (c) HF/3-21G* electrostatic potential isosurface (isovalue = −35 kcal mol^{-1}) of 1,5-dimethoxynaphthalene.

and the geometries were optimized (HF/3-21G) at each step constraining both the angle θ and the centroid−centroid separation. The plot of the resulting binding energies ΔE against the angle θ shows (Figure 7b) a difference of 6.0 kcal mol^{-1} between the most stable orientation (θ = 10°) and the least favorable one (θ = 70°). The negative electrostatic potential presented (Figure 7c) by the methoxy oxygen atoms is best complemented by the highly electron-deficient pyridinium rings when the angle θ is 10°. A nearly perpendicular orientation (θ = 70°) of the O···O and N···N axes moves the negative and positive regions apart destabilizing the complex.

To establish the relative contribution of the $\pi-\pi$ stacking and [C−H···O] hydrogen-bonding interactions to the overall binding energy of the complex [1/5DN38C10][PQT]$^{2+}$, a series of single-point HF/3-21G calculations were performed on model compounds. The solid-state and calculated geometries of the complex [1/5DN38C10][PQT]$^{2+}$ were employed (Figure 6) individually as the model complex structures. The 1,5-dioxynaphthalene rings were deleted without altering the relative orientation of the remaining components. The resulting "complex" (**IV**) and its separate "host" (**V**) and "guest" (**VI**) components were subjected individually to single-point HF/3-21G calculations. Subtracting the calculated energy of **IV** from those of **V** and **VI** gave interaction energies[20] of −82 and −78 kcal mol^{-1} for the solid-state and calculated "parent" structures, respectively. *These large interaction energies result from the*

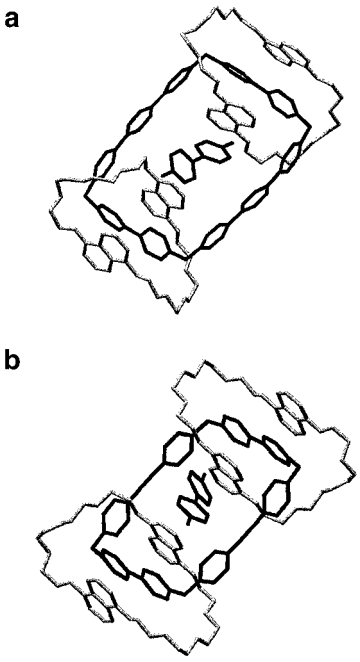

Figure 8. (a) Calculated (simulated annealing, AMBER* force field) geometry of the complex [**2**]$^{4+}$[PQT]$^{2+}$. (b) Calculated (PRCG minimization, AMBER* force field) geometry of the complex [**4**]$^{4+}$[PQT]$^{2+}$.

[C−H···O] hydrogen bonds. More precisely, the highly electron-deficient bipyridinium protons interact strongly with the negative electrostatic potential presented by the polyether oxygen atoms. Deleting the polyether chains instead (**I**−**III**, Figure 6) results in interaction energies[18] of −21 and −23 kcal mol^{-1} for the aromatic···aromatic interactions in the solid-state and calculated parent structures, respectively. *These interaction energies result from $\pi-\pi$ stacking interactions*. These observations suggest that *the contribution of the [C−H···O] hydrogen bonds to the overall binding energy is approximately 4 times higher than that associated with the $\pi-\pi$ stacking interactions!*[21] The interaction energies are enormous for the gas-phase calculations with a small basis set. Nevertheless, the very different magnitudes of [C−H···O] and [$\pi\cdots\pi$] interactions will be maintained in solution.

In a second set of model calculations, the solid-state structures provided by the single-crystal X-ray analyses of the [3]catenanes **2**$^{4+}$ and **4**$^{4+}$ were used to construct the complexes between each of the [3]catenanes and [PQT]$^{2+}$. These complexes were generated by introducing manually the guest into the cavities of the hosts with Macromodel.[17] The geometries of the resulting complexes were optimized by employing the PRCG algorithm,[22] and then they were subjected to simulated annealing using the AMBER* force field and the GB/SA solvation model for H_2O. The global minimum found (Figure 8a) for the complex [**2**]$^{4+}$[PQT]$^{2+}$ shows the guest to be inserted through the cavity of the [3]catenane. By contrast, in the case of **4**$^{4+}$, the guest is

(20) No significant differences were observed in the values of the interaction energies when these were calculated with the inclusion of chloride counterions.

(21) A similar effect was observed experimentally in a series of related pseudorotaxanes incorporating bipyridinium and 1,4-dioxybenzene recognition sites: (a) Anelli, P. L.; Ashton, P. R.; Ballardini, R.; Balzani, V.; Delgado, M.; Gandolfi, M. T.; Goodnow, T. T.; Kaifer, A. E.; Philp, D.; Pietraszkiewicz, M.; Prodi, L.; Reddington, M. V.; Slawin, A. M. Z.; Spencer, N.; Stoddart, J. F.; Vicent, C.; Williams, D. J. *J. Am. Chem. Soc.* **1992**, *114*, 193-218. (b) Asakawa, M.; Brown, C. L.; Menzer, S.; Raymo, F. M.; Stoddart, J. F.; Williams, D. J. *J. Am. Chem. Soc.* **1997**, *119*, 2614−2627.

(22) Polak, E.; Ribiere, G. *Rev. Fr. Inf. Rech. Oper.* **1969**, *16-R1*, 35−43.

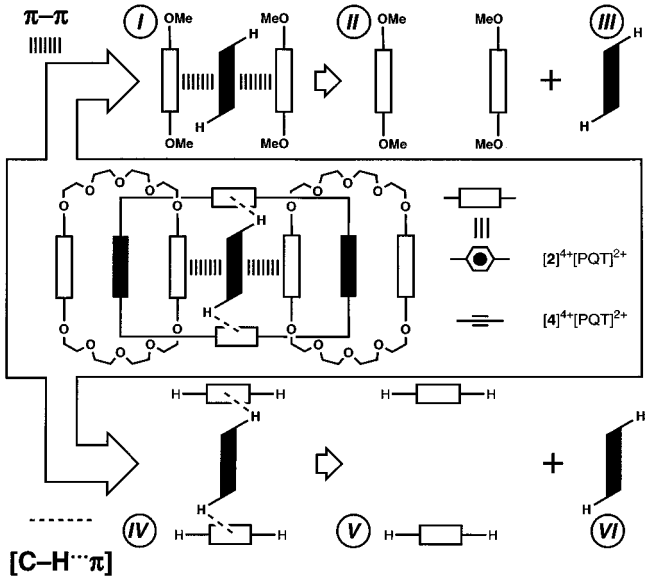

Figure 9. Fragmentation of the complexes $[\mathbf{2}]^{4+}[PQT]^{2+}$ and $[\mathbf{4}]^{4+}[PQT]^{2+}$ performed in order to "isolate" the [C−H···π] from the $\pi-\pi$ stacking interactions.

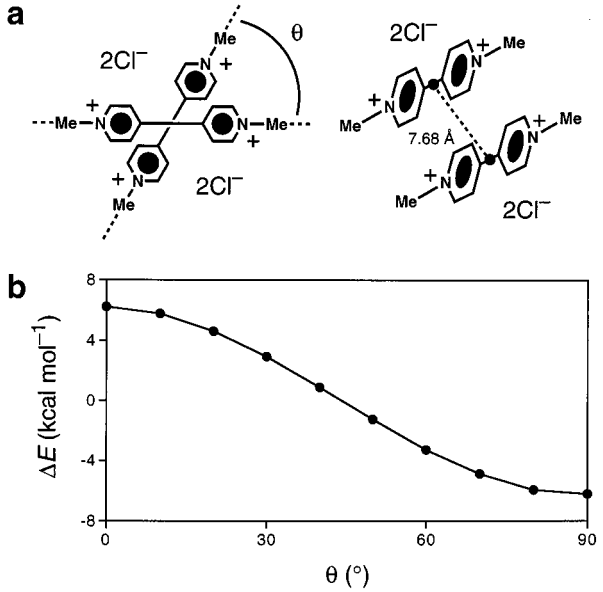

Figure 10. (a) The model dimer complex employed to evaluate the effect of the relative orientation of the bipyridinium units on the binding energy. (b) Plot of the calculated (single point, HF/3-21G*) binding energies of a model dimer complex against the angle θ.

expelled from the cavity of the [3]catenane and the global minimum obtained shows the guest well-separated from the host.

The geometry calculated for the complex $[\mathbf{2}]^{4+}[PQT]^{2+}$ suggests that the hydrogen atoms in the α-positions with respect to the nitrogen atoms on the bipyridinium units may be engaged in [C−H···π] interactions with the central aromatic ring of the terpenylene spacers of the [3]catenane. To compare the relative contribution of these [C−H···π] interactions with that arising from the $\pi-\pi$ stacking interactions to the binding event, the geometry of $[\mathbf{2}]^{4+}[PQT]^{2+}$ calculated by simulated annealing was employed as the "parent" structure from which a series of model compounds (**I**−**VI**, Figure 9) were generated with Spartan. Once again, the $[PQT]^{2+}$ guest and the central aromatic rings of the terphenylene spacers were extracted from the "parent" structure, while their relative orientations were maintained. The energies of this "complex" (**IV**) and of its separate "host" (**V**) and "guest" (**VI**) components were derived by performing single-point HF/3-21G* calculations on each species. *The resulting energy difference*[20] *(−16 kcal mol*$^{-1}$*) arises mainly from favorable [C−H···π] interactions*. Similarly (**I**−**III**, Figure 9), the contribution of the $\pi-\pi$ stacking interactions[20] (−22 kcal mol^{-1}) was determined. The same procedure was applied to $[\mathbf{4}]^{4+}[PQT]^{2+}$ by employing the geometry (Figure 8b) calculated after the PR/CG minimization as the "parent" structure. Values of −10 and −16 kcal mol^{-1} were obtained[20] for the [C−H···π] and $\pi-\pi$ stacking interactions, respectively. Thus, on going from the complex $[1/5DN38C10][PQT]^{2+}$ to $[\mathbf{2}]^{4+}[PQT]^{2+}$ and $[\mathbf{4}]^{4+}[PQT]^{2+}$, the $\pi-\pi$ stacking interactions remain almost unaltered. However, *the [C−H···O] hydrogen bonds are lost in favor of [C−H···π] interactions, which are more than 4 times weaker*.

In addition to the decrease of stabilization energy arising from the loss of [C−H···O] hydrogen bonds in favor of weaker [C−H···π] interactions, the complex formation between the tetracationic [3]catenanes $\mathbf{2}^{4+}$ and $\mathbf{4}^{4+}$ and the dicationic guest $[PQT]^{2+}$ might be disfavored also by repulsive electrostatic interactions between the charged bipyridinium units of host and guest. To analyze the effect of these interactions, a model dimer complex composed of two identical $[PQT][Cl]_2$ units (Figure 10a) was employed. The geometry of $[PQT][Cl]_2$ was optimized at the HF/3-21G level, and then two $[PQT][Cl]_2$ units were oriented, within the build mode of Spartan, parallel to each other with a centroid−centroid separation of 7.68 Å—i.e., the distance separating the bipyridinium unit of the guest from one of the bipyridinium units of the host in the complex $[\mathbf{2}]^{4+}[PQT]^{2+}$ shown in Figure 8a. The angle θ was varied from 0 to 90° in consecutive steps of 10° each, and single-point HF/3-21G calculations were perfomed at each step. The plot of the resulting binding energies ΔE against the angle θ shows (Figure 10b) that energetically unfavorable orientations lie in the region between 0 and 45°. By contrast, energetically favorable orientations are achieved when the value of θ is between 45 and 90°. However, the associated interaction energies are significantly lower than those calculated (vide supra) for the [C−H···O], [$\pi\cdots\pi$], and [C−H···π] interactions, suggesting that their contribution to the overall binding energy is relatively small.

Conclusions

To construct multiply interlocked [4]catenanes, we have devised a two-stage self-assembly approach involving the formation of [3]catenane intermediates possessing internal cavities sufficiently large to allow the subsequent interlocking of a fourth macrocyclic component. These [3]catenanes incorporate two 1,5-dioxynaphthalene macrocyclic components and one tetracationic cyclophane component composed of two bipyridinium recognition sites separated by two long spacers—namely, terphenyl or tolan units. Surprisingly, however, the expected [4]catenanes were not obtained and only the [3]-catenane intermediates were isolated. Their single-crystal X-ray analyses, indeed, revealed the presence of large cavities lined by π-electron-rich 1,5-dioxynaphthalene units which seem to be ideal for the inclusion of π-electron-deficient bipyridinium-based guests. However, the solution ^{1}H NMR and UV−vis spectra of the [3]catenanes did not change significantly upon the addition of either $[PQT][PF_6]_2$ or $[DQT][PF_6]_2$. A computational investigation indicates that the loss of favorable [C−H···O] hydrogen-bonding interactions prevents complex formation. The magnitude of these interactions is very large. The precise evaluation of the magnitude of these effects, now known to be much greater than originally appreciated, are under

evaluation in our laboratories. The importance of such [C−H···O] interactions continues to be illustrated in many biological situations and manifested in supramolecular systems.

Experimental Section

General Procedures. Solvents were dried according to literature methods.[23] Dimethylformamide (DMF) was distilled from calcium hydride under reduced pressure, and acetonitrile (MeCN) was distilled from calcium hydride under an atmosphere of N_2. Tetrahydrofuran (THF) was refluxed over sodium acetophenone ketal and distilled under N_2. 4,4′-Dimethyl-*p*-terphenyl **6**,[24] 4,4′-dimethyl-*p*-phenylacetylene **10**,[25] and 1,5-dioxynaphtho-38-crown-10 (1/5DN38C10)[14] were prepared according to literature procedures. Reactions requiring ultrahigh pressures were carried out in Teflon vessels using a custom-built ultrahigh-pressure reactor manufactured by PSIKA Pressure Systems Limited, Glossop, UK. Thin-layer chromatography (TLC) was performed on aluminum plates coated with Merck 5554 Kieselgel 60 F_{254}. The plates were air-dried and examined under a UV lamp and, then, if necessary, developed in an iodine vapor tank. Column chromatography was performed using Kieselgel 60 (0.040−0.063 mm mesh, Merck 9385). Melting points were determined using an Electrothermal 9200 melting point apparatus and are uncorrected. UV−visible spectra were recorded at 25 °C on a Perkin-Elmer Lambda 2 spectrophotometer fitted with a thermostated cell holder and operating under microcomputer control. Electron impact mass spectroscopy (EIMS) was carried out on either a Kratos Profile or a VG Prospec instrument. Liquid secondary ion mass spectrometry (LSIMS) was carrried out on a VG Zabspec mass spectrometer. ^{1}H nuclear magnetic resonance (NMR) spectra were recorded on either a Bruker AC300 (300 MHz) or a Bruker AMX400 (400 MHz) spectrometer using the deuterated solvent as lock and the residual solvent as an internal reference. ^{13}C NMR spectra were recorded on a Bruker AC300 (75 MHz) spectrometer using the JMOD pulse sequence (assuming $^1J_{CH}$ = 143 Hz) or the PENDANT sequence. Elemental analyses were performed by the University of Sheffied Microanalytical Service.

4,4′-Bis(bromomethyl)-1,4-terphenyl, 7.[26] 4,4′-Dimethyl-1,4-terphenyl, **6** (0.52 g, 2 mmol), and *N*-bromosuccimide (NBS) (0.79 g, 4.4 mmol) were suspended in CCl_4 (50 mL) and heated under reflux. AIBN was added in catalytic amounts over a period of 2.5 h. After being cooled to room temperature, the mixture was filtered, and the solid residues were washed with boiling CCl_4 (5 × 30 mL). The solvent was then evaporated under reduced pressure, and the product was recrystallized from $MeCO_2Et$ twice to afford a white crystalline solid (0.3 g, 40%): mp 102−104 °C (lit.[27] 265 °C, PhMe); LSIMS *m*/*z* 416 $[M]^+$; ^{1}H NMR (300 MHz, $CDCl_3$, 300 K) δ 7.68 (s, 4H), 7.62−7.60 (m, 4H), 7.50−7.48 (m, 4H), 4.58 (s, 4H).

4,4′-Bis(4,4′-pyridylpyridiniumylmethyl)-1,4′-terphenyl Bis(hexafluorophosphate), 5·2PF$_6$. 4,4′-Bipyridine (0.63 g, 4 mmol) was dissolved in MeCN (200 mL), and the solution was heated under reflux. Then, the dibromide **7** (0.2 g, 0.5 mmol) was added gradually as a solid in increasing amounts over a period of 8 h. After being cooled to room temperature, the mixture was filtered. The resulting solid was dissolved in 100 mL of Me_2CO/H_2O (1:1, v/v), and a concentrated solution of NH_4PF_6 in H_2O was added gradually until no further precipitate was observed. The precipitate was filtered off and washed with H_2O, Et_2O, and $CHCl_3$ to afford **5**·2PF_6 as a white powder (0.16 g, 60%): dec >280 °C, LSIMS *m*/*z* 713 $[M - PF_6]^+$; ^{1}H NMR [300 MHz, $(CD_3)_2CO$, 300 K] δ 9.51−9.46 (m, 4H), 8.90−8.87 (b m, 4H), 8.74−8.71 (m, 4H), 8.05−8.00 (b m, 4H), 7.91−7.88 (m, 12H), 6.23 (s, 4H); ^{13}C NMR (75 MHz, $CDCl_3$, 300 K) δ 155.2, 152.4, 145.8, 142.4, 141.4, 140.1, 133.0, 130.6, 128.6, 128.4, 127.1, 122.7, 64.6. Anal. Calcd for $C_{40}H_{32}F_{12}N_2P$**2**·HPF_6·H_2O: C, 45.36; H, 3.35; N, 5.29. Found: C, 45.68; H, 3.14; N, 5.38.

[3]Catenane 2·4PF$_6$. Method A. The bis(hexafluorophosphate) salt **5**·2PF_6 (50 mg, 0.06 mmol), the dibromide **6** (24 mg, 0.06 mmol), and the macrocyclic polyether 1/5DN38C10 (140 mg, 0.22 mmol) suspended in MeCN (10 mL) were stirred for 2 weeks at ambient temperature. The mixture was filtered, and the solvent was removed in vacuo. The resulting red solid was purified by column chromatography [SiO_2, 2 M NH_4Cl/MeOH/$MeNO_2$ (7:2:1, v/v/v)]. The fractions containing the desired product were combined, and the solvent was evaporated under reduced pressure. The residue was dissolved in H_2O, and a saturated aqueous solution of NH_4PF_6 was added to afford a red precipitate. Crystallization of the resulting red solid by vapor diffusion of *i*-Pr_2O into a MeCN solution of the product gave the [3]catenane **2**·4PF_6 as a red crystalline solid (6 mg, 4%): dec >210 °C; HRMS *m*/*z* (LSIMS) calcd for $[M - PF_6]^+$ $C_{132}H_{136}F_{18}N_4O_{20}P_3$, 2531.8673, found 2531.8732; LSIMS *m*/*z* 2534 $[M - PF_6]^+$, 2389 $[M - 2PF_6]^+$, 2244 $[M - 3PF_6]$; ^{1}H NMR (300 MHz, CD_3CN, 300 K) δ 8.75−8.69 (b d, 8H), 7.75 (d, 8H), 7.85 (d, 8H), 7.53 (s, 8H), 6.68 (d, 8H), 6.55−6.35 (b t, 8H), 6.23 (d, 8H), 5.84 (s, 8H), 3.98−3.74 (m, 64H). Crystals suitable for X-ray crystallographic analysis were grown by vapor diffusion of *i*-Pr_2O into a MeCN solution of the [3]catenane. Crystal data: $C_{132}H_{136}N_4O_{20}$·4PF_6·4H_2O, M = 2822.46, monoclinic, a = 22.239(3) Å, b = 12.223(2) Å, c = 28.287(5) Å, β = 95.69(1)°, V = 7651(2) Å^3, space group $P2_1/c$, Z = 2 (the structure has crystallographic C_i symmetry), D_c = 1.225 g cm^{-3}, μ(Cu Kα) = 1.271 mm^{-1}, λ = 1.541 78 Å, F(000) = 2944. Data for a crystal having dimensions of 0.35 × 0.23 × 0.18 mm were measured on a Siemens P4/RA diffractometer with Cu Kα radiation (graphite monochromated) using ω scans at 293 K. Of the 9595 independent reflections measured ($\theta \leq$ 55°), 5697 had $I_o > 2\sigma(I_o)$ and were considered to be observed. The data were corrected for Lorentz and polarization effects, but not for absorption. The structure was solved by direct methods. One PF_6^- counterion was disordered and subsequently split into two half-occupied positions. The ΔF maps showed the presence of unidentified solvent molecules. These were refined as partially occupied H_2O molecules. Hydrogen atoms for the H_2O molecules were not located; all other hydrogen atoms were placed in idealized positions with U_{eq}(H) = 1.2U_{eq}(C) and were allowed to ride on their parent atoms. Anisotropic refinement for all non-hydrogen atoms, with the exception of those of the partially occupied H_2O molecules, gave R_1 = 0.1253 and wR_2 = 0.3384. All computations were carried out using the SHELXTL 5.03 package. Atomic coordinates and bond lengths and angles have been deposited at the Cambridge Crystallographic Data Centre.

Method B. The bis(hexafluorophosphate) salt **5**·2PF_6 (50 mg, 0.06 mmol), the dibromide **6** (24 mg, 0.06 mmol), and the macrocyclic polyether 1/5DN38C10 (140 mg, 0.22 mmol) were dissolved in DMF (7 mL), and the solution was subjected to a pressure of 12 kbar for 2 days at ambient temperature. The solvent was evaporated, and the resulting residue was purified as described in method A to afford the [3]catenane **2**·4PF_6 (20 mg, 15%).

4,4′-Bis(bromomethyl)tolan, 10.[27] 4,4′-Bis(methyl)tolan (0.42 g, 2 mmol) and *N*-bromosuccimide (NBS) (0.79 g, 4.4 mmol) were suspended in CCl_4 (50 mL), the mixture was heated and heated under reflux. AIBN was added in catalytic amounts over a period 2.5 h. After being cooled to room temperature, the mixture was filtered, and the solid residue was washed with boiling CCl_4 (5 × 30 mL). The solvent was evaporated under reduced pressure, and the product was recrystallized from $MeCO_2Et$ twice to afford a white crystalline solid (0.4 g, 55%): mp 110−112 °C (lit.[28] 187−190 °C, benzene); LSIMS *m*/*z* 416 $[M]^+$; ^{1}H NMR (300 MHz, $CDCl_3$, 300 K) δ 7.55−7.50 (m, 4H), 7.47−7.83 (m, 4H), 4.58 (s, 4H).

4,4′-Bis(4,4′-pyridylpyridiniumylmethyl)tolan Bis(hexafluorophosphate), 8·2PF$_6$. 4,4′-Bipyridine (1.70 g, 10.89 mmol) was dissolved in MeCN (200 mL), and the solution was heated under reflux. The dibromide **10** (1.98 g, 5.45 mmol) was added gradually as a solid in increasing amounts over a period 8 h. After being cooled to room temperature, the mixture was filtered. The resulting solid was dissolved in 100 mL of Me_2CO/H_2O (1:1, v/v), and a concentrated solution of NH_4PF_6 in H_2O was added until no further precipitate was observed.

(23) Furniss, B. S.; Hannaford, A. J.; Smith, P. W. G.; Tatchell, A. R. *Practical Organic Chemistry*; Longman: New York, 1989.
(24) Hart, H.; Harada, K.; Du, C. J. F. *J. Org. Chem.* **1985**, *50*, 3104−3110.
(25) Tao, W.; Nesbitt, S.; Heck, R. F. *J. Org. Chem.* **1990**, 55, 63−69.
(26) Helm, A.; Heiler, D.; McLendon, G. *J. Am. Chem. Soc.* **1992**, *114*, 6227−6238.
(27) Raston, I.; Wennerstroem, O. *Acta Chem. Scand.* **1982**, *36*, 655−660.

The precipitate was filtered-off and washed with H_2O, Et_2O and $CHCl_3$ to afford the **8**·2PF_6 as a white powder (2.19 g, 50%). mp dec > 280 °C; LSIMS *m/z* 1467 [2M-PF_6]$^+$, 661 [M − PF_6]$^+$; ^{1}H NMR [300 MHz, $(CD_3)_2CO$, 300 K] d 8.85−8.75 (m, 8H), 8.38−8.75 (m, 4H), 7.85−8.78 (m, 4H), 7.77−7.74 (bm, 4H), 7.51−7.40 (m, 4H), 6.23 (s, 4H); ^{13}C NMR (75 MHz, $CDCl_3$, 300 K) d 157.2, 152.1, 146.0, 142.1, 134.4, 133.4, 130.6, 127.3, 125.2, 64.7, 52.3,; Anal.calcd for $C_{36}H_{28}F_{12}N_2P_2$: C 53.60, H 3.47, N 6.95; found C 53.43, H 3.38, N 6.85.

[3]Catenane 4·4PF_6. Method A. The bis(hexafluorophosphate) salt **8**·2PF_6 (78 mg, 0.096 mmol), the dibromide **10** (35 mg, 0.096 mmol), and the macrocyclic polyether 1/5DN38C10 (154 mg, 0.24 mmol) suspended in MeCN (10 mL) were stirred for 2 weeks at ambient temperature. The mixture was filtered and the solvent removed in vacuo. The resulting red solid was purified by column chromatography [SiO_2, 2 M NH_4Cl/MeOH/$MeNO_2$ (7:2:1, v/v/v)], which gave two different products. Each product was dissolved in H_2O, and a saturated aqueous solution of NH_4PF_6 was added to afford a red precipitate. Crystallization of the two products by vapor diffusion of benzene into MeCN solutions of the compounds gave a [2]catenane (15 mg, 10%) and the [3]catenane **4**·4PF_6 (25 mg, 35%). [2]Catenane: dec >210 °C; HRMS *m/z* (LSIMS) calcd for [M − PF_6]$^+$, $C_{88}H_{84}F_{18}N_4O_{10}P_3$, 1791.5113, found 1791.5162; LSIMS *m/z* 1937 [M]$^+$, 1792 [M − PF_6]$^+$, 1647 [M − 2PF_6]$^+$, 1502 [M − 3PF_6]$^+$; ^{1}H NMR (300 MHz, CD_3CN, 300 K) δ 8.78−8.72 (m, 8H), 7.80−7.55 (m, 16H), 6.62−6.51 (m, 4H), 6.29−6.20 (m, 4H), 6.10−5.85 (m, 4H), 5.75 (s, 8H), 4.10−3.90 (m, 32H). [3]Catenane **4**·4PF_6: dec >210 °C; HRMS *m/z* (LSIMS) calcd for [M − PF_6]$^+$, $C_{124}H_{128}F_{18}N_4O_{20}P_3$, 2427.8047, found 2427.8025; LSIMS *m/z* 2574 [M]$^+$, 2429 [M − PF_6]$^+$, 2284 [M − 2PF_6]$^+$, 2139 [M − 3PF_6]$^+$; ^{1}H NMR (300 MHz, CD_3CN, 300 K) δ 8.75−8.69 (b d, 8H), 7.75 (d, 8H), 7.85 (d, 8H), 7.65 (s, 8H), 6.68 (d, 8H), 6.55−6.47 (b t, 8H), 6.20 (d, 8H), 5.74 (s, 8H), 3.99−3.76 (m, 64H). Crystals suitable for X-ray crystallographic analysis were grown by vapor diffusion of MeOH into a MeCN solution of the [3]catenane. Crystal data: $C_{124}H_{128}N_4O_{20}$·4PF_6·4MeCN·4MeOH, M = 2802.48, monoclinic, a = 13.152(5) Å, b = 14.344(3) Å, c = 22.034(9) Å, α = 98.98(2)°, β = 95.62(3)°, γ = 103.21(2)°, V = 3959(2) Å^3, space group $P\bar{1}$, Z = 1 (the structure has crystallographic C_i symmetry), D_c = 1.175 g cm^{-3}, μ(Cu Kα) = 1.205 mm^{-1}, λ = 1.54178 Å, F(000) = 1460. Data for a crystal having dimensions of 0.50 × 0.33 × 0.20 mm were measured on a Siemens P4/RA diffractometer with Cu Kα radiation (graphite monochromated) using ω scans at 203 K. Of the 7976 independent reflections measured ($\theta \leq 50°$), 5740 had $I_o > 2\sigma(I_o)$ and were considered to be observed. The data were corrected for Lorentz and polarization effects but not for absorption. The structure was solved by direct methods. Solvent molecules found in the structure are disordered: two MeCN molecules distributed over four positions and two MeOH over four positions. Hydrogen atoms were placed in idealized positions with U_{eq}(H) = 1.2U_{eq}(C) and U_{eq}(H) = 1.5U_{eq}(Me) and were allowed to ride on their parent atoms. Anisotropic refinement for all non-hydrogen atoms, with the exception of those of the partially occupied MeOH, gave R_1 = 0.1178 and ωR_2 = 0.3166. All computations were carried out using the SHELXTL 5.03 package. Atomic coordinates and bond lengths and angles have been deposited at the Cambridge Crystallographic Data Centre.

Method B. The bis(hexafluorophosphate) salt **8**·2PF_6 (78 mg, 0.1 mmol), the dibromide **10** (35 mg, 0.1 mmol), and the macrocyclic polyether 1/5DN38C10 (154 mg, 0.24 mmol) were dissolved in DMF (7 mL), and the solution was subjected to a pressure of 12 kbar for 2 days at ambient temperature. The solvent was evaporated, and the resulting residue was purified as described in method A to afford the [2]catenane (21 mg, 15%) and the [3]catenane **4**·4PF_6 (87 mg, 35%).

Molecular Modeling. The solid-state structure of the complex [1/5DN38C10][PQT]$^{2+}$ was employed as the initial geometry. The complexes [**2**]$^{4+}$[PQT]$^{2+}$ and [**4**]$^{4+}$[PQT]$^{2+}$ were constructed within the input mode of Macromodel 5.0[17] by employing the solid-state structures of the [3]catenanes as the initial geometries and then docking manually the guest inside their cavities. All complexes with and without chloride counterions were subjected to energy minimization employing the Polak-Ribiere Conjugate Gradient (PRCG) method,[22] the AMBER* force field,[15] and the Generalized-Born Surface Area (GB/SA) solvation model[16] for H_2O, as implemented in Macromodel 5.0. The optimized geometries were subjected individually to simulated annealing performed by employing the AMBER* force field, the GB/SA solvation model for H_2O, and the PRCG minimization algorithm. The temperature was gradually decreased from 500 to 50 K in 10 consecutive molecular dynamics steps of 20.0 ps each. The bath constant and the time step were mantained at 5.0 ps and 1.5 fs, respectively, in all steps. All HF/3-21G* calculations were perfomed by using Spartan 4.1[18] and model complexes and compounds generated after appropriate fragmentations (**I**−**VI**, Figures 7 and 10) of the output structures of the simulated annealing, in the case of [1/5DN38C10][PQT]$^{2+}$ and [**2**]$^{4+}$[PQT]$^{2+}$, or of the energy minimization, in the case of [**4**]$^{4+}$[PQT]$^{2+}$, [1/5DN38C10]-[PQT][Cl]$_2$, [**2**][PQT][Cl]$_6$, and [**4**][PQT][Cl]$_6$.

Acknowledgment. This research was supported by the Engineering and Physical Sciences Research Council, U.K., and by the National Institute of General Medical Sciences, National Institutes of Health.

Supporting Information Available: Partial ^{1}H NMR spectra, additional structural diagrams, and tables listing atomic coordinates, temperature factors, bond lengths and angles, and torsion angles. This material is available free of charge on the Internet at http://pubs.acs.org.

JA982748B